Immunoelectron Microscopic Localization of Neural Cell Adhesion Molecules (L1, N-CAM, and Myelin-associated Glycoprotein) in Regenerating Adult Mouse Sciatic Nerve

Rudolf Martini and Melitta Schachner

Department of Neurobiology, University of Heidelberg, 69 Heidelberg, Federal Republic of Germany

Abstract. The localization of the neural cell adhesion molecules L1, N-CAM, and the myelin-associated glycoprotein was studied by pre- and postembedding staining procedures at the light and electron microscopic levels in transected and crushed adult mouse sciatic nerve. During the first 2–6 d after transection, myelinated and nonmyelinated axons degenerated in the distal part of the proximal stump close to the transection site and over the entire length of the distal part of the transected nerve. During this time, regrowing axons were seen only in the proximal, but not in the distal nerve stump. In most cases L1 and N-CAM remained detectable at cell contacts between nonmyelinating Schwann cells and degenerating axons as long as these were still morphologically intact. Similarly, myelin-associated glycoprotein remained detectable in the periaxonal area of the degenerating myelinated axons. During and after degeneration of axons, nonmyelinating Schwann cells formed slender processes which were L1 and N-CAM positive. They resembled small-diameter axons but could be unequivocally identified as Schwann cells by chronical denervation. Unlike the nonmyelinating Schwann cells, only few myelinating ones expressed L1 and N-CAM. At the cut ends of the nerve stumps a cap developed (more at the proximal than at the distal stump) that contained S-100–negative and fibronectin-positive fibroblast-like cells. Most of these cells were N-CAM positive but always L1 negative. Growth cones and regrowing axons expressed N-CAM and L1 at contact sites with these cells. Regrowing axons of small diameter were L1 and N-CAM positive where they made contact with each other or with Schwann cells, while large-diameter axons were only poorly antigen positive or completely negative.

14 d after transection, when regrowing axons were seen in the distal part of the transected nerve, regrowing axons made L1- and N-CAM–positive contacts with Schwann cells. When contacting basement membrane, axons were rarely found to express L1 and N-CAM. Most, if not all, Schwann cells associated with degenerating myelin expressed L1 and N-CAM. In crushed nerves, the immunostaining pattern was essentially the same as in the cut nerve. During formation of myelin, the sequence of adhesion molecule expression was the same as during development: L1 disappeared and N-CAM was reduced on myelinating Schwann cells and axons after the Schwann cell process had turned ~1.5 loops around the axon. Myelin-associated glycoprotein then appeared both periaxonally and on the turning loops of Schwann cells in the uncompacted myelin.

We infer from these observations that L1 and N-CAM are involved in supporting axon regrowth on the surface of Schwann and fibroblast-like cells, and that, after the initial contacts between axons and Schwann cells, regulation of adhesion molecule expression during regeneration in many ways recapitulates development.

In contrast to lower vertebrates, mammals show very poor neuronal regeneration in the adult central nervous system (Ramon y Cajal, 1928*b*). In the peripheral nervous system of mammals, however, regrowth of severed axons of both peripheral and central nervous system origin succeeds over considerable distances (Aguayo, 1985; Ramon y Cajal, 1928*a*; Tello, 1911, as cited in Ramon y Cajal, 1928*b*). Schwann cells, the glia of the peripheral nervous system, are uniquely endowed to permit this regrowth, whereas central nervous system glia of adult but not of developing mammals prohibit functional axonal regrowth (Aguayo, 1985; Ramon y Cajal, 1928*b*; Smith et al., 1986). The cellular and molecular mechanisms underlying this unique capacity have remained unknown but are likely to depend at least to some extent on cell surface interactions between regrowing axons and glial environment.

Cell surface molecules that are involved in recognition between different cell types and, therefore, operationally termed cell adhesion molecules have recently been implicated in neuron–glia interactions. They are thus possible candidates for the guidance of axons along adhesive pathways during development (Silver and Rutishauser, 1984). Whether adhesion molecules are involved in neuronal regeneration is presently unknown. The neural cell adhesion molecules L1 and N-CAM have both been shown to be involved in neuron–Schwann cell adhesion (Seilheimer, B., E. Persohn, and M. Schachner, manuscript in preparation) and may, therefore, support axon outgrowth on Schwann cells. L1, which is immunochemically identical to the nerve growth factor–inducible large external glycoprotein NILE, which in turn is identical to Ng-CAM (Bock et al., 1985; Friedlander et al., 1986), is increased by nerve growth factor in its expression not only on neurons, but also on Schwann cells (Seilheimer and Schachner, 1987). While contact between neurons and Schwann cells is, on one hand, mediated by cell adhesion molecules, expression of L1 and N-CAM is, on the other, influenced by cell contact with neurons (Seilheimer, B., E. Persohn, and M. Schachner, manuscript in preparation). These observations suggest a considerable degree of regulatory signals that influence cell adhesion molecule expression by Schwann cells.

The present study was undertaken to investigate the expression of neural cell adhesion molecules in the injured peripheral nervous system of adult mice in situ to gain insights into their function during regeneration. In addition, it seemed pertinent to compare, at the ultrastructural level, the sequence and localization of cell adhesion molecule expression between development (Martini and Schachner, 1986) and regeneration (Nieke and Schachner, 1985; Daniloff et al., 1986).

Materials and Methods

Immunocytology

Indirect immunoelectron microscopy was carried out by preembedding and postembedding staining procedures, as described previously (Martini and Schachner, 1986), with the only exception being that the tissue used for the postembedding technique was fixed with 2% paraformaldehyde and 2% glutaraldehyde in 0.12 M Palay buffer (Palay and Chan-Palay, 1974). For indirect immunofluorescence, cryo-sections (10 μm thick) were cut from nerve stumps frozen in liquid nitrogen and fixed for 15 min at room temperature in 4% paraformaldehyde, then washed in PBS pH 7.3, followed by 95% ethanol/5% acetic acid for 10 min at −20°C. Sections were then processed for indirect immunofluorescence essentially as described (Goridis et al., 1978; Schnitzer et al., 1981). Appropriate controls for light and electron immunocytology have also been described (Martini and Schachner, 1986; Nieke and Schachner, 1985). Production and immunoaffinity purification of polyclonal antibodies to L1, N-CAM, and myelin-associated glycoprotein (MAG)[1] have also been described (Martini and Schachner, 1986). Antibodies to vimentin were prepared according to Franke et al. (1979) and obtained from W. W. Franke (Deutsches Krebsforschungszentrum, Heidelberg). Polyclonal antibodies to fibronectin were prepared as described (Schachner et al., 1978). Antibodies to S-100 protein were obtained from DAKOPATTS (Copenhagen) and from R. Mirsky, University College, London.

Quantitation of Gold Particles on Ultrathin Sections

Areas of 40–80 μm^2 were selected in micrographs of ultrathin sections labeled by the immunogold postembedding staining technique. Gold particles associated with surface membranes were counted, the length of the surface membrane was measured with a turn and bank indicator, and the density of gold particles per μm was calculated.

Lesioning of Sciatic Nerve

NMRI mice (males and females, 8–12 wk old) were bred and maintained at the departmental animal facility. Mice were anesthetized by ether inhalation. The sciatic nerve of one side was exposed in the thigh region and transected with small scissors or crushed with forceps for 20 s. For chronic denervation, the gap between proximal and distal stumps was increased by removing a 10-mm-long piece and by sewing the proximal stump to the skin. The nerve of the other side was left intact for control. After the operation the skin was sewn with 2–3 stitches. For immunocytology, animals were perfused (Martini and Schachner, 1986) at intervals of 2, 4, 5, 6, 14, 22, 45, and 150 d after operation. At each interval, 4–6 animals were investigated.

Results

Sciatic nerves of adult mice were transected or crushed, and localization of the neural cell adhesion molecules L1, N-CAM, and MAG was followed by immunocytology at the light and electron microscopic levels at various time intervals after placing the lesion.

Transected Nerve

2–6 d after Transection. During the first 2–6 d after transection, different stages of degenerating axons and myelin were observed in the distal stump along its entire length and in the distal region of the proximal stump of the transected nerve.

1. *Abbreviation used in this paper*: MAG, myelin-associated glycoprotein.

Figure 1. Immunocytological localization at light (*a*) and electron (*d–g*) microscopic levels of N-CAM (*a*, *d*, and *e*), L1 (*g*), and fibronectin (*f*) in the proximal stump of adult mouse sciatic nerve 4 (*d*), 5 (*e* and *f*), and 6 (*a–c*) d after transection. Immunocytology at the light microscopic level was performed by indirect immunofluorescence and by electron microscopy by pre- (*d*) and postembedding (*e–g*) staining procedures. (*a*) Fibroblast-like cells in the cap at the proximal nerve stump and nerve fibers within the endoneurium are N-CAM positive. The locations of the cap and endoneurium are indicated in the corresponding phase-contrast micrograph (*b*). (*b*) Corresponding phase-contrast micrograph to fluorescence image (*a*). Broken line indicates the boundary between the cap (*C*) on the left and endoneurium (*E*) on the right of the proximal stump. Arrow points to the distal end of the stump. (*c*) Negative control showing a section stained for indirect immunofluorescence with second antibody only. (*d*) Fibroblast-like cell (*F*) in the cap at the cut end of the proximal nerve stump is N-CAM positive on its surface. Arrows point to electron-dense reaction product. Extracellular matrix is not stained (*arrowhead*). Ribosomes around the endoplasmic reticulum are not visible because the section has not been counterstained. (*e*) N-CAM–positive fibroblast-like cell (*F*) as in *d*. Note the immunogold labeling associated with the rough endoplasmic reticulum (*circled gold particles*) and on the surface membrane (*arrows*). (*f*) Fibroblast-like cell (*F*) as in *d* and *e* is associated with fibronectin-positive exracellular matrix (*arrowheads*). Labeling is also associated with rough endoplasmic reticulum (*circled gold particles*). Note "empty" vacuoles (*asterisks*) which are electron dense when osmification has preceded dehydration in preembedded tissue (see Fig. 2 *a*). (*g*) Contact between thin axonal processes (*asterisks*) and thick axonal sprouts (*Ax*) are L1 positive. Where thick axons make contact with each other labeling is weak (*arrow*). Contact between thick axon and Schwann cell (*S*) is not stained in this case. Bars: (*a–c*) 20 μm; (*d–g*) 0.25 μm.

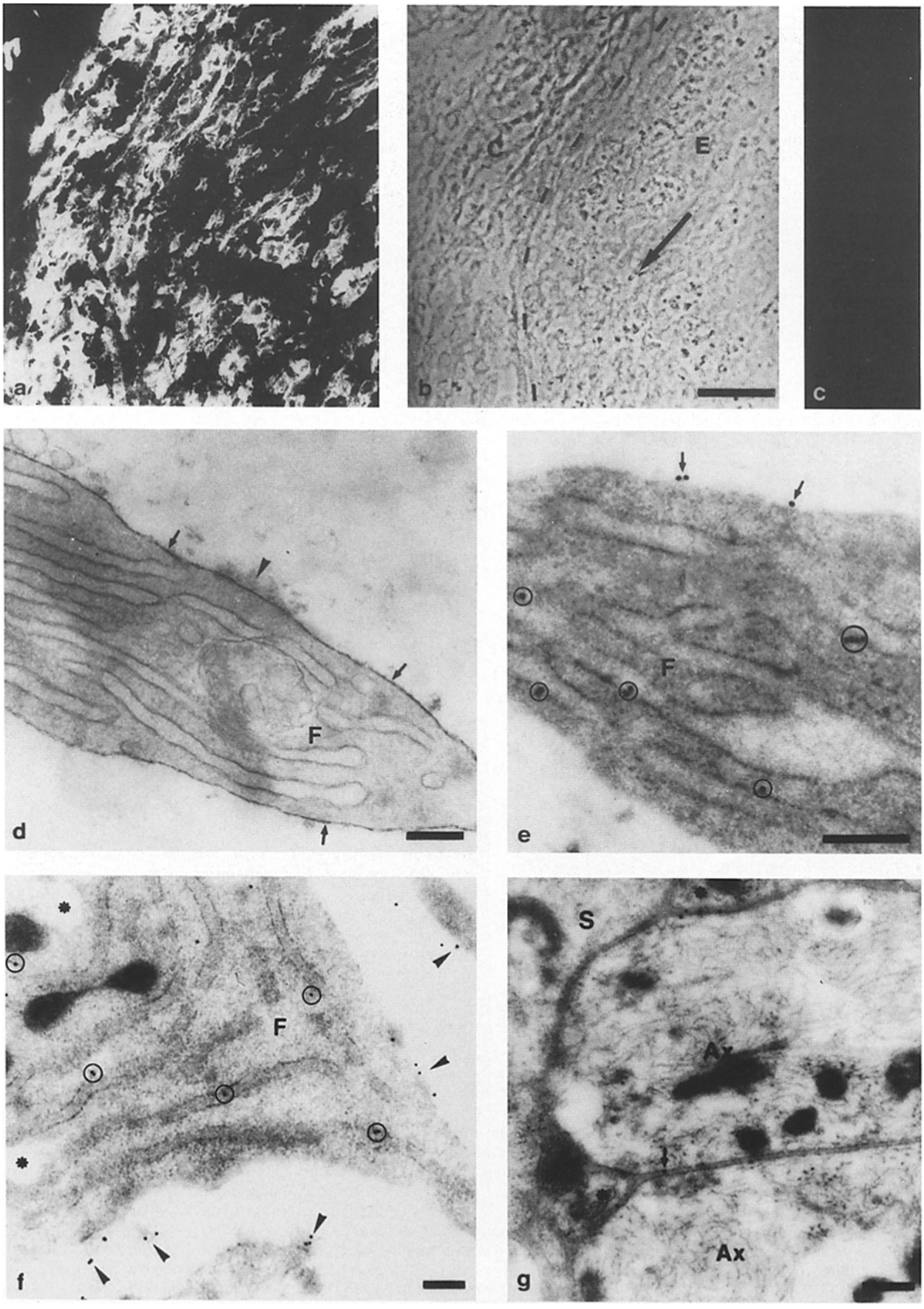

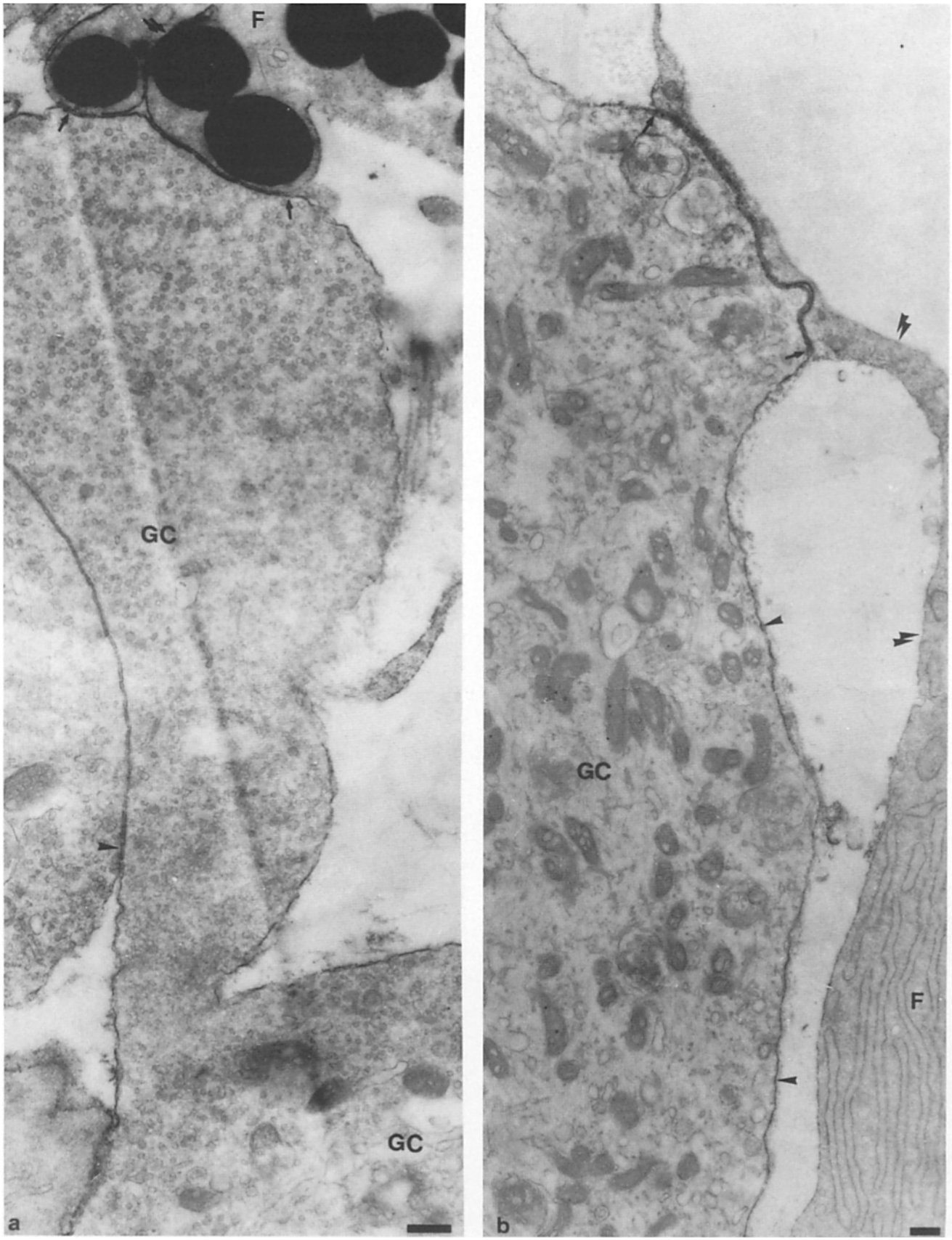

Figure 2. Immunoelectron microscopic localization of N-CAM (*a*) and L1 (*b*) on growth cones contacting fibroblast-like cells in the cap at the cut end of the proximal sciatic nerve stump 4 d after transection. Staining was performed by preembedding procedures. Immunoperoxidase reaction product is indicated by arrows. (*a*) Note N-CAM positivity at the contact sites between growth cone lobe (*GC*) and fibroblast-

Table I. Quantitation of Immunogold Labeling Density

Type of cellular structures	L1	MAG
Contact between fasciculating small-diameter axons	2.06 ± 0.86(20)	0.00 ± 0.00(10)
Contact between fasciculating large-diameter axons	0.13 ± 0.18(20)	0.00 ± 0.00(10)
Contact between unmyelinated small-diameter axon and nonmyelinating Schwann cell	1.75 ± 0.79(20)	0.00 ± 0.00(15)
Contact between myelinated axon and myelin sheath	0.00 ± 0.00(20)	2.80 ± 1.55(10)
Contact between Schwann cells in distal stump, 14 or more d after transection	1.21 ± 0.43(15)	0.00 ± 0.00(10)
Contact between growth cone and Schwann cell or fibroblast-like cell	1.64 ± 0.80(10)	–
Surface of growth cone not in contact	0.20 ± 0.45(5)	–

Numbers represent gold particles/μm associated membrane (mean values ± SD). Numbers of micrographs analyzed of at least three independent experiments with cut nerves at different times after transection are given in brackets. All values above 1.0 are significantly different from those below ($P < 0.05$). It should be noted that growth cones are sometimes difficult to discern from "giant axons" by postembedding staining procedures.

In addition to the degenerating axons, live nonmyelinated axons covering a range in diameter between 1 and 2 μm and <0.5 μm were visible in the proximal nerve stump. Small-diameter axons tended to form bundles or surround single large-diameter axons. These bundles and the large-diameter axons were mostly seen associated with processes of Schwann cells. Large-diameter axons also were associated with other large-diameter axons or, more frequently, with small-diameter axons. These intact axons are probably the terminal sprouts and collaterals of regenerating axons, since segmental demyelination during retrograde degeneration has not been observed previously (Morris et al., 1972*a*). Growth cones were very rarely observed. When they were seen, they contacted Schwann cells or fibroblast-like cells near the cut.

Myelinating and nonmyelinating Schwann cells in distal and proximal nerve stumps were observed with slender processes which contacted other Schwann cell processes or, in the proximal stump, regrowing large- and small-diameter axons. Since Schwann cell processes contained microtubules and intermediate filaments, they were often difficult to distinguish from regrowing axons, especially at stages later than 6 d after lesioning when regrowth had occurred. However, since these processes were also seen in chronically denervated nerve stumps, they could be identified as Schwann cells. In addition, they were stained by antibodies to the intermediate filament protein vimentin, which is not present in differentiated axons.

At the cut end of both nerve stumps (i.e., the most proximal part of the distal stump and the most distal part of the proximal stump) spindle- and star-shaped cells formed an ~200–400-μm-long cap across the cut nerve (Fig. 1 *b*). Their cell bodies and their long processes contained many osmiophilic vacuoles and extensive rough endoplasmic reticulum. These cells did not stain with antibodies to the Schwann cell marker protein S-100 at the light microscopic level (not shown) and were always associated with strongly fibronectin-positive extracellular matrix constituents (Fig. 1 *f*) and are, therefore, believed to be fibroblast-like cells (Cornbrooks et al., 1983). A further indication of the fibroblast-like character of these cells is their occasional association with the unraveling perineurial sheath. Apart from the fibroblast-like cells, many macrophages and few unidentified cells, possibly Schwann cells, were observed in the distal part of the proximal stump.

Polyclonal antibodies to L1 and N-CAM showed a similar staining pattern on most cellular structures as it had been previously observed during development (Martini and Schachner, 1986). In the proximal stump, prominent immunostaining for L1 and N-CAM was seen at cell surface contacts between cell surfaces of slender processes of unmyelinated Schwann cells. Contact sites were also antigen positive when the slender Schwann cell processes touched upon small- and large-diameter axons. Cell contacts were always L1 and N-CAM positive when small-diameter axons were associated with each other in bundles or when small-diameter axons were in contact with large-diameter ones (Fig. 1 *g*). However, when large-diameter axons were associated with each other, L1 and N-CAM were hardly detectable (Fig. 1 *g*). Growth cones were L1 and N-CAM positive, particularly at contact sites between L1- and N-CAM–positive Schwann cells or even L1-negative fibroblast-like cells (Fig. 2, *a* and *b*). This characteristic staining pattern was also obtained with the immunogold technique where leakage of the peroxidase reaction product is avoided (see also Table I). It is our impression that growth cone surfaces were relatively weakly stained with L1 and N-CAM antibodies where they do not contact other cells (Fig. 2, *a* and *b*). The fibronectin-positive fibroblast-like cells in the cap at the transected site were L1 negative and most often, but interestingly not always, N-CAM positive (Fig. 1, *a*, *d*, and *e*, and Fig. 2 *b*). N-CAM and fibronectin were recognizable in these cells in the rough endoplasmic reticulum (Fig. 1, *e* and *f*). Endoneurial, epineurial, and perineurial fibroblasts outside the caps were never L1 or N-CAM positive and contacted by L1- or N-CAM–positive growth cones or axons. Not only fibronectin, but also L1 and, more weakly, N-CAM were occasion-

like cell (*F*) (surface membranes between *arrows*) and between processes of a fibroblast-like cell (*double arrow*). Contacts between growth cones are only very weakly labeled (*arrowhead*). (*b*) Strong L1 positivity is confined to contacts between growth cone (*GC*) and fibroblast-like cell (*F*) (surface membranes between *arrows*), whereas growth cone without cell contact is weakly stained (*arrowheads*). Fibroblast-like cell appears L1 negative (*double arrowheads*). Bars, 0.25 μm.

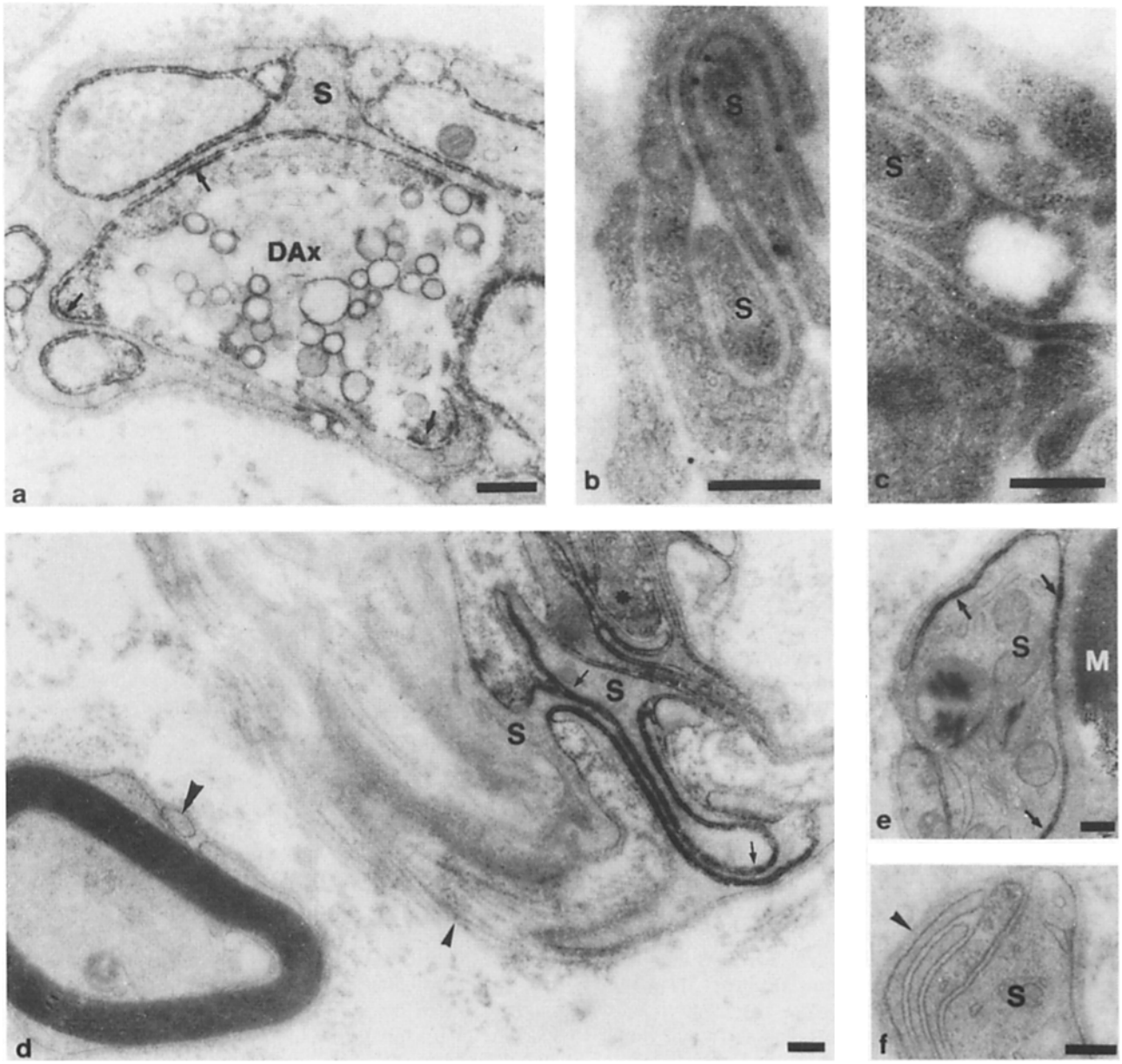

Figure 3. Immunoelectron microscopic localization of L1 (*a*, *b*, *d*, *e*) and appropriate negative controls (*c* and *f*) in the distal stumps of the transected (*a*, *d–f*) and chronically denervated (*b* and *c*) sciatic nerve, 2 (*a*), 4 (*d* and *f*), and 14 (*b*, *c*, and *e*) d after operation. Staining was performed by pre- (*a*, *d*, *e*, and *f*) and postembedding (*b* and *c*) procedures. (*a*) Contact between nonmyelinating Schwann cell (*S*) and degenerating axon (*DAx*) is L1 positive which is indicated by arrows pointing to electron-dense reaction product. (*b*) L1-positive Schwann cell processes (*S*) in the chronically denervated nerve. Note gold particles associated with cell contact sites. (*c*) Negative control of the chronically denervated nerve which was only treated with gold-conjugated second antibody. No gold particles are visible. *S*, Schwann cell processes. (*d*) Processes of a nonmyelinating Schwann cell (*S*) are L1 positive as indicated by electron-dense reaction product (*arrows*). The myelinating Schwann cell does not express detectable levels of L1 (*large arrowhead*). Contact between a nonmyelinated degenerating axon (*asterisk*) and nonmyelinating Schwann cell processes (*S*) is L1 negative. Collagen fibrils are also L1 negative (*small arrowhead*). (*e*) Processes of a myelinating Schwann cell (*S*) are densely stained and therefore L1 positive at contacts with each other (*arrows*). *M*, degenerating myelin. (*f*) Negative control treated with polyclonal antibodies to human hemoglobin and subsequently with peroxidase-coupled second antibodies. No electron-dense reaction product is visible. Basement membrane is indicated by arrowhead. *S*, Schwann cell. Bars, 0.25 μm.

ally seen associated with the basement membrane and interstitial collagens in both the distal and proximal nerve stumps. Macrophages did not express detectable levels of L1 or N-CAM.

In the distal part of the transected nerve most slender processes of unmyelinated Schwann cells in contact with each other were L1 and N-CAM positive (Fig. 3 *d*). The Schwann cell origin of these slender processes was confirmed by immunostaining for vimentin (not shown) or chronical denervation (Fig. 3, *b* and *c*). L1 and N-CAM were not detectable on processes of myelinating Schwann cells 2 d after transection. 4–6 d after transection only 10–20% of all Schwann cells associated with degenerating myelin showed L1 and N-CAM on their cell processes (Fig. 3 *d*). In most

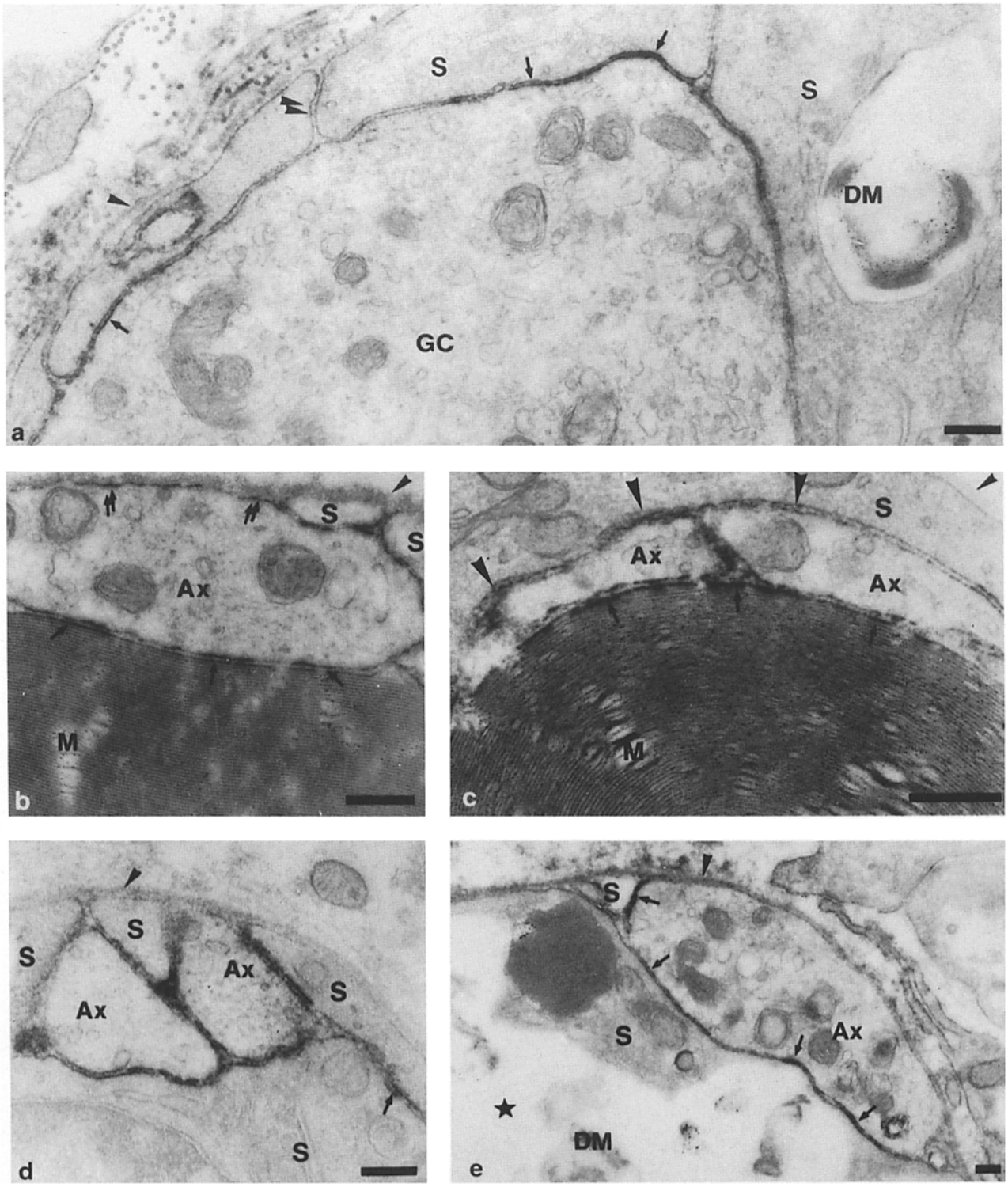

Figure 4. Immunoelectron microscopy of the distal part of the crushed (*a–c*, and *e*) and transected (*d*) sciatic nerve 4 (*a–c*, and *e*) and 14 (*d*) d after operation. L1 (*a*, *b*, *d*, and *e*) and N-CAM (*c*) staining was done by preembedding procecdures. Stained membranes are covered by an electron-dense reaction product. (*a*) Growth cone (*GC*) makes L1-positive contact with Schwann cell (*arrows*). Schwann cell processes (*S*) are not yet labeled at this stage (*double arrowheads*). Degenerating myelin of the Schwann cell (*DM*); weakly stained basement membrane (*arrowhead*). (*b*) Regrowing axon (*Ax*) makes L1-positive contact with basement membrane (*double arrows*), Schwann cell processes (*S*), and the reasonably intact myelin sheath (*M*). Basement membrane is also positive for L1 (*arrowhead*). (*c*) Two regenerating axons (*Ax*) as in *b*. N-CAM is detectable at contacts of axons with each other and with a Schwann cell (*S*, *large arrowheads*). N-CAM is also present at the contact sites between axons and myelin (*M*, *arrows*). Basement membrane is unstained (*small arrowhead*). (*d*) L1-positive cell contacts between regrowing axons (*Ax*) and a Schwann cell (*S*). Note the absence of electron-dense staining where axon touches the basement membrane. L1-positive contact between Schwann cell processes (*arrow*) (cf. Fig. 4 *a*); very weakly stained basement membrane (*arrowhead*). (*e*) Axon (*Ax*) grows between outer Schwann cell membrane and the L1-positive basement membrane (*arrowhead*). L1 is localized at the contact sites between axon and Schwann cell (*arrows*). The axolemma associated with the inner aspect of the basement membrane is not L1 positive. *DM*, degenerating myelin; *S*, Schwann cell; *, "empty" vacuole probably from degenerated myelin. Bars, 0.25 μm.

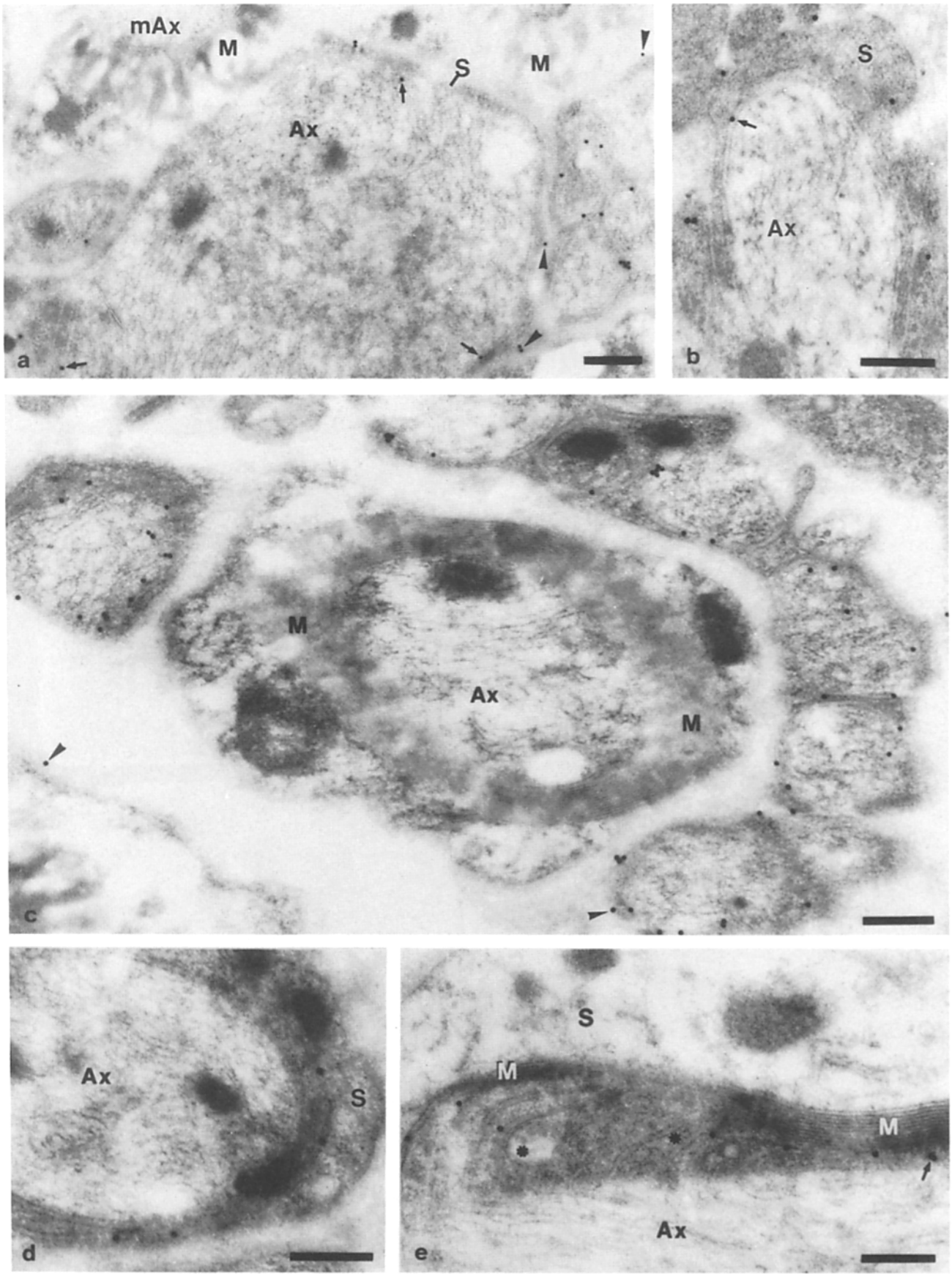

Figure 5. Immunoelectron microscopic localization of L1 (*a*, and *c*), N-CAM (*b*), and MAG (*d* and *e*) in the distal (*b* and *e*) and proximal (*a*, *c* and *d*) part of a transected sciatic nerve 22 d after operation. Immunogold labeling was performed by postembedding procedures. (*a*) Contact between a large-diameter axon (*Ax*) and Schwann cell envelope (*S*) is L1 positive (*arrows*) at the onset of myelination. More

cases, cell contact between degenerating nonmyelinated small-diameter axons and Schwann cells were L1 and N-CAM positive even at more advanced stages of degeneration when the axolemma had broken up and the axoplasm vacuolized (Fig. 3 *a*). Similar observations were made for MAG which remained detectable at the axon–myelin interface as long as axon–myelin contacts were intact (not shown). MAG was very rarely detected on endoneurial collagens or basement membrane by the postembedding staining technique.

14–22 d after Transection. 14–22 d after transection, regeneration units consisting of small- and large-diameter axons could be observed in the proximal nerve stump. In these regeneration units all stages of remyelination were visible: unmyelinated axons, axons in the process of myelination, and axons surrounded by compact myelin.

In the distal nerve stumps most myelin sheaths had disappeared. At 14 d after transection, the first regrown axons were detectable between the outer Schwann cell membrane and the basement membrane. Axons were also found ensheathed by Schwann cells. Only few (mostly fasciculating) axons were seen outside the Schwann cell tubes or within empty Schwann cell basement membranes. Newly formed compact myelin was first seen at ~22 d after transection. At this time the developmental range of nonmyelinated to fully myelinated axons was present in the distal stump.

In the distal and proximal nerve stumps, N-CAM and L1 were detectable on both nonmyelinated axons and nonmyelinating Schwann cells (Figs. 4 *d*, and 5, *a–c*). In contrast to less advanced regenerative stages, the few Schwann cells still associated with degenerating myelin were always L1 and N-CAM positive (Fig. 3 *e*). At the onset of myelination, when the Schwann cell had enveloped the axon ~1.5–2 times, L1 was no longer detectable at contact sites between axons and Schwann cells. At this stage of myelination, N-CAM was seen only at low levels but remained detectable periaxonally and even more weakly in compact myelin. Another difference between L1 and N-CAM immunostaining was that N-CAM was more detectable at contacts of Schwann cells with each other than at the nonmyelinated axon–Schwann cell contact (Fig. 5 *b*). MAG was first detectable when the Schwann cell process had turned around the axon ~2 times (Fig. 5 *d*). At later stages of myelin formation, MAG was seen in the periaxonal interface and in the uncompacted portions of myelin (Fig. 5 *e*).

In the distal stump, cell contacts between regrowing axons and outer Schwann cell membranes were L1 and N-CAM positive (Fig. 4 *d*). Interestingly, contacts between axons and basement membranes were weakly or not L1 and N-CAM positive (Fig. 4 *d*). Cell contacts between fasciculating axons were always L1 and N-CAM positive. Basement membranes of Schwann cells and interstitial collagen fibers of the endoneurium were L1, N-CAM, and MAG positive in some areas, but not in others. No correlation between stage of regeneration and staining of basement membrane could be observed.

45 and 150 d after Transection. At these advanced stages of regeneration, myelinated axons were drastically increased in number in both the distal nerve stump and distal part of the proximal stump. The main differences between these stages of a regenerating nerve and a normal untransected nerve were the thinner myelin sheaths, persisting slender Schwann cell processes, and a larger number of nonmyelinated and myelinated axons.

The staining pattern of these structures with antibodies to L1, N-CAM, and MAG was the same as at the less advanced stages of remyelination.

For quantitation of immunolabeling intensities gold particles associated with the surface membranes were counted (Table I). The values determined were in agreement with the description in the previous paragraphs obtained by pre- and postembedding staining methods. The values observed for N-CAM were similar to those of L1 except that contacts between axon and myelin sheath were labeled (0.72 ± 0.38 gold particles/μm determined from 10 [*n*] micrographs). Also, staining of contacts between unmyelinated axons and Schwann cells was significantly lower (0.67 ± 0.42, $n = 10$) than between Schwann cell processes (1.53 ± 0.77, $n = 10$; $P < 0.05$).

Crushed Nerve

Nerve crush experiments were performed to increase the chance for finding growth cones in the distal part of the injured nerve. Since axons have been known to regrow in a more coordinated fashion after crush, many more growth cones should be found in a particular area. Almost all axons that had regrown distally from the crush were found within Schwann cell tubes; i.e., within the confines of the basement membranes of the Schwann cells. Most axons grew individually or as bundles between the Schwann cell and its basement membrane, or were surrounded by Schwann cells. Axons preferred contacts with Schwann cells over those with basement membranes only. This was even the case for Schwann cell tubes, in which the basement membrane was only very partially covered by Schwann cell processes. Most growth cones were found in close contact with Schwann cells, but often growth cones were also found in contact with fasciculating axons. When compact myelin was still present in the Schwann cell tube, regenerating fibers sometimes made contact with the outer surface of the myelin sheath. Once myelin had degenerated, regrowing axons never used the inner Schwann cell membrane formerly associated with myelin.

Distally from the crush, cell contacts between axons and Schwann cells were L1 and N-CAM positive (Fig. 4, *b*, *c*, and *e*). L1 and N-CAM were also seen at axon contacts with the outer loops of compact myelin (Fig. 4, *b* and *c*). Contacts between axons and basement membranes were rarely L1 and

intense staining is seen around small-diameter axons which are ensheathed by a nonmyelinating Schwann cell. Compact myelin (*M*) and myelinated fibers (*mAx*) are not labeled. Basement membrane is L1 positive (*arrowheads*). (*b*) Single axon (*Ax*) associated with a Schwann cell envelope (*S*) is N-CAM positive. Contacts between Schwann cell processes are more N-CAM positive than between axon and Schwann cell. (*c*) Part of a "regeneration unit" in the proximal stump with unmyelinated axons, probably collaterals of the L1-negative myelinated axon (*Ax*) being strongly L1 positive. Basement membrane is L1 positive (*arrowheads*). *M*, compact myelin. (*d*) MAG is detectable on myelin-forming Schwann cell membrane when the mesaxon has enveloped the axon (*Ax*) about two times. *S*, cytoplasm of the myelin-forming Schwann cell. (*e*) MAG is detectable in the region of the paranodal loops (*asterisks*) and between axon and compact myelin (*arrow*). Compact myelin (*M*) is MAG negative. *S*, cytoplasm of the Schwann cell. Bars, 0.25 μm.

never N-CAM positive (Fig. 4 *b*). Basement membranes themselves were sometimes also L1 and N-CAM positive (Fig. 4, *b* and *e*). Contacts of growth cones with Schwann cells were always L1 and N-CAM positive but staining intensities were generally somewhat weaker than on the axon itself (Fig. 4 *a*). Cell contacts between growth cones and fasciculating axons were intensely labeled with L1 antibodies. As observed in transected nerves, contacts between processes of myelinating Schwann cells were often L1 and N-CAM negative in the distal stumps 4–6 d after placing the lesion (Fig. 4 *a*).

Discussion

Since one aim of the present study was to compare the expression of adhesion molecules between regeneration and development, a summary of the similarities and differences in cell–cell interactions between the two conditions seems warranted. During development, the bulk of the peripheral axons are believed to pass through Schwann cell-free territory in the initial phases of outgrowth, whereas during regeneration axons encounter an environment which consists of Schwann cells, fibroblasts, macrophages, and the extracellular matrix structures of basement membrane and endoneurial collagens. Whether, in development, Schwann cells precede and are responsible for successful axon outgrowth in the more distal parts of the periphery is a possibility that would make regeneration more similar to development (for review, see Keynes, 1987). However, since Schwann cells are believed to synthesize extracellular matrix only after contact with neurons (Bunge et al., 1986), an organized basement membrane is not likely to be responsible for axon outgrowth during development. In contrast, during regeneration the basement membranes of residual Schwann cell tubes of live and killed denervated peripheral nerves have been reported to be important pathways for regrowing axons (Ide et al., 1983; Schwab and Thoenen, 1985). It is pertinent in this context that the basement membrane constituents, laminin and a heparan sulfate proteoglycan, have been suggested to support neuron regeneration in vivo (Chiu et al., 1986). It has, however, recently been shown that a crucial ingredient for neurite regrowth is the availability of living cells in the distal nerve stump (Hall, 1986).

In several investigations dealing with the regeneration of peripheral nerves at the ultrastructural level, axons and growth cones have been shown not to grow exclusively along the inner aspect of the basement membrane, but additionally to contact living Schwann cells (Barton, 1962; Kuffler, 1986; Nathaniel and Pease, 1963; Scherer and Easter, 1984; Schwab and Thoenen, 1985). When grafts of the peripheral and central nervous systems have been killed by freezing and thawing before implanting into the transected peripheral nerves, living Schwann cells from the host could be observed to migrate into the grafts and are preferably used for contact by growth cones and axons (Anderson and Turmaine, 1986; Ide et al., 1983). When axons grew within relatively empty tubes of Schwann cell basement membrane, they often showed the tendency to make contact with cell surfaces of living cells, such as Schwann cells or other axons (Ide et al., 1983; Schwab and Thoenen, 1985). Also in our investigation we have always observed axons that were at least partly in contact with living Schwann cells or other axons and never exclusively only with basement membrane. It is, therefore, interesting that in cases where axon–basement membrane contacts could be observed, this contact tended to be less L1 and N-CAM positive than the contact between axon and Schwann cell. It is quite evident from our study, however, that the axon prefers the contact of Schwann cells at the Schwann cell–basement membrane interface and not at the site that was previously in contact with axons. Interestingly, regrowing axons sometimes also make L1- and N-CAM–positive contacts with myelin fragments when these are still reasonably intact. It is likely that this type of interaction results from a possibly less preferred contact between axon and basement membrane or the inability of axons to grow over long distances on basement membrane alone. The latter feature is interesting from the point of view that in the developing (Martini and Schachner, 1986) as well as in the regenerating sciatic nerve, the extracellular matrix was found to be positive for L1 and N-CAM in some areas, but not in others. During regeneration, we could not observe any correlation of adhesion molecule expression in the extracellular matrix with a particular state of axon regrowth. We would, therefore, like to speculate that the patchy, noncontinuous expression of adhesion molecules is hardly capable of supporting regrowth of axons. Instead, our observations support the view that the basement membrane alone is not solely responsible for axon regrowth and that surface membranes perform crucial functions in neuronal regeneration. This view is in agreement with the observations of Tomaselli et al. (1986) on the promotion of axonal growth on Schwann cells not only by extracellular matrix constituents, but also by extractable surface membrane constituents.

A particular feature of the regrowing axon is the reduced expression of L1 and N-CAM on growth cones, especially when not in contact with other cells. Although we have not rigorously quantified L1 and N-CAM expression on growth cones vs. their axonal shafts, these differences are apparent both by pre- and postembedding staining techniques. A relatively high expression of N-CAM has previously been observed on growth cones in cell culture (van den Pol et al., 1986). However, the authors were not able to distinguish whether the labeling was increased where the growth cones contacted other cells due to antibody penetration problems in the culture system. Recently, growth cones of cultured neuroblastoma cells have been observed to express higher levels of N-CAM 140 than N-CAM 180. N-CAM 180 is the larger component of N-CAM with the longest cytoplasmic domain that (*a*) is linked to the cytoskeleton, (*b*) has a reduced lateral mobility within the surface membrane, and (*c*) has thus been suggested to be involved in stabilization of cell contacts (Pollerberg et al., 1986, 1987). These "free," searching growth cones were not associated with prominent N-CAM 180 and L1 expression. However, when growth cones were seen in contact with other cells, they showed an increased expression of N-CAM 180 and L1 (Pollerberg et al., 1987). From these observations, it is tempting to speculate that a reduced detectability of N-CAM and L1 on growth cones in situ is characteristic of their state of active growth which might be hindered by higher concentrations of adhesive molecules. Conversely, stabilization of contacts between the axon shaft and its cellular environment would be mediated by the more prominent expression of L1 and N-CAM.

Of particular interest is the expression of N-CAM in the

fibronectin-positive and S-100–negative fibroblast-like cells of the cap at the cut ends of the distal and proximal nerve stumps that was also observed by Daniloff et al. (1986). These fibroblast-like cells have not been observed to be L1 positive in the present study in contrast to our previous observations at the light microscopic level (Nieke and Schachner, 1985). It is possible that L1 detectability in the cap (in our previous publication) was due to regrowth of L1-positive axons. Although morphological and immunocytochemical data suggest that the N-CAM–positive cells are fibroblast-like cells, we cannot rule out that some of these cells are derived from Schwann cells (for a detailed discussion about the metaplasia between fibroblasts and Schwann cells, see Morris et al., 1972*b*). The occurence of N-CAM on these fibroblast-like cells is interesting from the point of view that axons regrow through this territory after transection (Ramon y Cajal, 1928*a*). Furthermore, fibroblast-like cells in endo-, epi- and perineurium are never N-CAM positive, neither during postnatal development nor in the normal adult state. They also have not been observed to be N-CAM positive outside the cap during regeneration. It is therefore tempting to speculate that the expression of N-CAM in the cap is involved in mediating regrowth of axons. A possibly similar situation is seen in muscle where the number of interstitial, fibroblast-like cells increases drastically after denervation at the original synaptic sites (Connor et al., 1987). At least some of these cells express N-CAM and thus might be involved in reinnervation of the muscle (Covault and Sanes, 1985). The molecular and cellular signals that underlie the expression of N-CAM in these cells and the fibroblast-like cells of the cap remain to be determined.

Adhesion molecule expression during development has recently been studied by immunohistological methods at the light and electron microscopic levels (Martini and Schachner, 1986; Nieke and Schachner, 1985; Rieger et al., 1986). The investigations from our laboratory have focused on the consecutive expression of different cell adhesion molecules during myelin formation in developing sciatic nerves and shall therefore serve as reference for the regenerating nerve. At birth, the earliest time point tested in our developmental study, all Schwann cells are highly L1 and N-CAM positive in their proliferative state and when in contact with each other and with axons. Interestingly, basement membranes and interstitial collagens are not adhesion molecule positive at this stage. Axons, which are mostly fasciculating ones, are also strongly L1 and N-CAM positive. With the onset of myelination after Schwann cells have turned ~1.5 times around axons, L1 ceases to be detectable on axons and Schwann cells. N-CAM, in contrast, remains detectable, although at reduced levels at the axon–Schwann cell interface and in compact myelin. MAG appears periaxonally after the Schwann cell has turned ~1.5–2 loops around the axon and, interestingly, is also apparent at the surfaces of the turning loops of the Schwann cell. In the compact myelin, MAG is no longer present, but remains detectable in the uncompacted regions of outer and inner mesaxon, Schmidt–Lanterman incisures, and paranodal loops. These observations point to a very intricate temporal and spatial regulation of the three adhesion molecules during the process of myelination.

During degeneration few myelinating Schwann cells revert to an L1- and N-CAM–positive state within 4–6 d after transection of the nerve in the distal stumps. However, 14 d after transection, most, if not all, Schwann cells still associated with degenerating myelin are L1 and N-CAM positive. Whether this reexpression of L1 and N-CAM is triggered by a preceding Schwann cell proliferation (Abercrombie and Johnson, 1946) will have to be determined. Comparison of crushed and transected nerves has shown that axon regrowth into the distal stump is independent of detectable expression of L1 and N-CAM by Schwann cells and that reexpression of these molecules on Schwann cells in not triggered by axonal contact. With the onset of myelination, however, L1 and N-CAM undergo a regulation of expression on both axons and Schwann cells that is reminiscent of development. L1 ceases to be expressed on both partners at the onset of myelination when the turning loops of Schwann cells have progressed 1.5 times around the axon. N-CAM is also reduced in its expression periaxonally but remains detectable during myelination not only at the axon–Schwann cell interface, but also in compact myelin. Also as in development, MAG appears exactly at the time L1 is lost periaxonally and on the myelinating Schwann cell. A feature not observed in development are the unmyelinated, poorly L1- and N-CAM–positive, large-diameter axons from which the small-diameter L1- and N-CAM–positive collaterals sprout. Although the regulatory signals underlying adhesion molecule expression in regenerating peripheral nerves need to be investigated and, in particular, related to development, our present observations would agree with the contention that adhesion molecule expression during regeneration in many ways recapitulates development.

The authors are grateful to Luitgard Freidel for technical assistance; T. Fahrig, W. W. Franke, B. Gehrig, R. Mirsky, and P. Pesheva for antibodies; W. Blakemore for a helpful suggestion.

The authors are grateful to Deutsche Forschungsgemeinschaft for support (postdoctoral fellowship to Rudolf Martini and Sonderforschungsbereich 317).

Received for publication 6 July 1987, and in revised form 6 January 1988.

References

Abercrombie, M., and M. L. Johnson. 1946. Quantitative histology of Wallerian degeneration: Nuclear population in rabbit sciatic nerve. *J. Anat.* 80:37–50.

Aguayo, A. J. 1985. Axonal regeneration from injured neurons in the adult mammalian central nervous system. *In* Synaptic Plasticity. C. W. Cotman, editor. The Guilford Press, New York. 457–484.

Anderson, P. N., and M. Turmaine. 1986. Peripheral nerve regeneration through grafts of living and freeze-dried CNS tissue. *Neuropathol. Appl. Neurobiol.* 12:389–399.

Barton, A. A. 1962. An electron microscope study of degeneration and regeneration of nerve. *Brain.* 85:799–808.

Bock, E., C. Richter-Landsberg, A. Faissner, and M. Schachner. 1985. Demonstration of immunochemical identity between the nerve growth factor-inducible large external (NILE) glycoprotein and the cell adhesion molecule L1. *EMBO (Eur. Mol. Biol. Organ.) J.* 4:2765–2768.

Bunge, R. P., M. B. Bunge, and C. F. Eldridge. 1986. Linkage between axonal ensheathment and basal lamina production by Schwann cells. *Annu. Rev. Neurosci.* 9:305–328.

Chiu, A. Y., W. D. Matthew, and P. H. Patterson. 1986. A monoclonal antibody that blocks the activity of a neurite regeneration-promoting factor: studies on the binding site and its localization in vivo. *J. Cell Biol.* 103:1383–1398.

Connor, E. A., and U. J. McMahan. 1987. Cell accumulation in the junctional region of denervated muscle. *J. Cell Biol.* 104:109–120.

Cornbrooks, C. J., D. J. Carey, J. A. McDonald, R. Timpl, and R. P. Bunge. 1983. In vivo and in vitro observations on laminin production by Schwann cells. *Proc. Natl. Acad. Sci. USA.* 80:3850–3854.

Covault, J., and J. R. Sanes. 1985. Neural cell adhesion molecule (N-CAM) accumulates in denervated and paralyzed skeletal muscles. *Proc. Natl. Acad. Sci. USA.* 82:4544–4548.

Daniloff, J. K., G. Levi, M. Grumet, F. Rieger, and G. M. Edelman. 1986.

Altered expression of neural cell adhesion molecules induced by nerve injury and repair. *J. Cell Biol.* 103:929–945.
Franke, W. W., E. Schmid, S. Winter, M. Osborn, and K. Weber. 1979. Widespread occurrence of intermediate-sized filaments of the vimentin-type in cultured cells from diverse vertebrates. *Exp. Cell Res.* 123:25–46.
Friedlander, D. R., M. Grumet, and G. M. Edelman. 1986. Nerve growth factor enhances expression of neuron-glia cell adhesion molecule in PC12 cells. *J. Cell Biol.* 102:413–419.
Goridis, C., J. Martin, and M. Schachner. 1978. Characterization of an antiserum to synaptic glomeruli from rat cerebellum. *Brain Res. Bull.* 3:45–52.
Hall, S. M. 1986. The effect of inhibiting Schwann cell mitosis on the reinnervation of acellular autografts in the peripheral nervous system of the mouse. *Neuropathol. Appl. Neurobiol.* 12:401–414.
Ide, C., K. Tohyama, R. Yokota, T. Nitatori, and S. Onodera. 1983. Schwann cell basal lamina and nerve regeneration. *Brain Res.* 288:61–75.
Keynes, R. J. 1987. Schwann cells during neural development and regeneration: leaders or followers? *Trends Neurosci.* 10:137–139.
Kuffler, D. P. 1986. Accurate reinnervation of motor end plates after disruption of sheath cells and msucle fibers. *J. Comp. Neurol.* 250:228–235.
Martini, R., and M. Schachner. 1986. Immunoelectron microscopic localization of neural cell adhesion molecules (L1, N-CAM, and MAG) and their shared carbohydrate epitope and myelin basic protein in developing sciatic nerve. *J. Cell Biol.* 103:2439–2448.
Morris, J. H., A. R. Hudson, and G. Weddell. 1972*a*. A study of degeneration and regeneration in the divided rat sciatic nerve based on electron microscopy. II. The development of the "regenerating unit", *Z. Zellforsch.* 124: 103–130.
Morris, J. H., A. R. Hudson, and G. Weddell. 1972*b*. A study of degeneration and regeneration in the divided rat sciatic nerve based on electron microscopy. IV. Changes in fascicular microtopography, perineurium and endoneurial fibroblasts. *Z. Zellforsch.* 124:165–203.
Nathaniel, E. J. H., and D. C. Pease. 1963. Degenerative changes in rat dorsal roots during Wallerian degeneration. *J. Ultrastruct. Res.* 9:511–532.
Nieke, J., and M. Schachner. 1985. Expression of the neural cell adhesion molecules L1 and N-CAM and their common carbohydrate epitope L2/HNK-1 during development and after transection of the mouse sciatic nerve. *Differentiation.* 30:141–151.
Palay, S. L., and V. Chan-Palay. 1974. Cerebellar Cortex. Cytology and Organization. Springer-Verlag, New York, Heidelberg, Berlin. 348 pp.
Pollerberg, E., K. Burridge, K. Krebs, S. Goodman, and M. Schachner. 1987. The 180 kD component of the neural cell adhesion molecule N-CAM is involved in cell-cell contacts and cytoskeleton-membrane interactions. *Cell Tissue Res.* 250:227–236.
Pollerberg, E., M. Schachner, and J. Davoust. 1986. Differentiation-state dependent surface mobilities of two forms of the neural cell adhesion molecule. *Nature (Lond.).* 324:462–465.
Ramon y Cajal, S. 1928*a*. Degeneration and Regeneration of the Nervous System. Vol. 1. R. M. May, translator and editor. Oxford University Press, London. 396 pp.
Ramon y Cajal, S. 1928*b*. Degeneration and Regeneration of the Nervous System. Vol. 2. R. M. May, translator and editor. Oxford University Press, London. 397–769.
Rieger, F., J. K. Daniloff, M. Pincon-Raymond, K. L. Crossin, M. Grumet, and G. M. Edelman. 1986. Neuronal cell adhesion molecules and cytotactin are colocalized at the Node of Ranvier. *J. Cell Biol.* 103:379–391.
Schachner, M., G. Schoonmaker, and R. O. Hynes. 1978. Cellular and subcellular localizations of LETS protein in the nervous system. *Brain Res.* 158: 149–158.
Scherer, S. S., and S. S. Easter. 1984. Degenerative and regenerative changes in the trochlear nerve of goldfish. *J. Neurocytol.* 13:519–565.
Schnitzer, J., W. W. Franke, and M. Schachner. 1981. Immunocytochemical demonstration of vimentin in astrocytes and ependymal cells of developing and adult mouse nervous system. *J. Cell Biol.* 90:435–447.
Schwab, M. E., and H. Thoenen. 1985. Dissociated neurons regenerate into sciatic but not optic nerve explants in culture irrespective of neurotrophic factors. *J. Neurosci.* 5:2415–2423.
Seilheimer, B., and M. Schachner. 1987. Regulation of neural cell adhesion molecule expression on cultured mouse Schwann cells by nerve growth factor. *EMBO (Eur. Mol. Biol. Organ.) J.* 6:1611–1615.
Silver, J., and U. Rutishauser. 1984. Guidance of optic axons in vivo by a preformed adhesive pathway on neuroepithelial endfeet. *Dev. Biol.* 106: 485–499.
Smith, G. M., R. H. Miller, and J. Silver. 1986. Changing role of forebrain astrocytes during development, regenerative failure, and induced regeneration upon transplantation. *J. Comp. Neurol.* 251:23–43.
Tomaselli, K. J., L. F. Reichardt, and J. L. Bixby. 1986. Distinct molecular interactions mediate neuronal process outgrowth on non-neuronal cell surfaces and extracellular matrices. *J. Cell Biol.* 103:2659–2672.
van den Pol, A. N., U. di Porzio, and U. Rutishauser. 1986. Growth cone localization of neural cell adhesion molecule on central nervous system neurons in vitro. *J. Cell Biol.* 102:2281–2294.